

UCSF

UC San Francisco Previously Published Works

Title

Reliability of a new scoring system for intraarticular mineralization of the knee: Boston University Calcium Knee Score (BUCKS)

Permalink

<https://escholarship.org/uc/item/5f10f6k9>

Journal

Osteoarthritis and Cartilage, 28(6)

ISSN

1063-4584

Authors

Guermazi, A
Jarraya, M
Lynch, JA
[et al.](#)

Publication Date

2020-06-01

DOI

10.1016/j.joca.2020.03.003

Peer reviewed



Published in final edited form as:

Osteoarthritis Cartilage. 2020 June ; 28(6): 802–810. doi:10.1016/j.joca.2020.03.003.

Reliability of A New Scoring System for Intraarticular Mineralization of the Knee: BUCKS (Boston University Calcium Knee Score)

Ali Guermazi¹, Mohamed Jarraya^{1,2}, John A Lynch³, David T Felson⁴, Margaret Clancy⁴, Michael Nevitt³, Cora E. Lewis⁵, James Torner⁶, Tuhina Neogi⁴

⁽¹⁾Department of Radiology, Boston University School of Medicine, Boston University, Boston MA

⁽²⁾Department of Radiology, Mercy Catholic Medical Center, Darby, PA

⁽³⁾Department of Epidemiology, University of California San Francisco, CA

⁽⁴⁾Department of Medicine, Boston University School of Medicine, Boston University, Boston MA

⁽⁵⁾Department of Epidemiology, University of Alabama at Birmingham, AL

⁽⁶⁾Department of Epidemiology, College of Public Health, University of Iowa, IA

Abstract

BACKGROUND: The role of intra-articular mineralization in osteoarthritis (OA) is unclear. Its understanding may potentially advance our knowledge of knee OA pathogenesis. We describe and assess the reliability of a novel computed tomography (CT) scoring system, the Boston University Calcium Knee Score (BUCKS) for evaluating intra-articular mineralization.

METHODS: We included subjects from the most recent study visit of the Multicenter Osteoarthritis Study (MOST) Study, a NIH-funded longitudinal cohort of community-dwelling older adults with or at risk of knee OA. All subjects underwent CT of bilateral knees. Each knee

Corresponding Author: Ali Guermazi, MD, PhD, Address: VA Boston Healthcare System, 1400 VFW Parkway, Suite 1B105, West Roxbury, MA 02132, USA, guermazi@bu.edu.

Author contributions:

AG: conception and design of the study, acquisition of data, collection and assembly of data, analysis and interpretation of data, drafting the article, and final approval of the version to be submitted.

MJ: Acquisition of data, analysis and interpretation of data, collection and assembly of data, drafting the article, and final approval of the version to be submitted.

JL: Technical and logistic support, statistical expertise, analysis and interpretation of data, revising the manuscript critically for important intellectual content, and final approval of the version to be submitted.

DF: obtaining the funding, conception and design of the study, analysis and interpretation of data, revising the manuscript critically for important intellectual content, and final approval of the version to be submitted.

MC: Administrative support, analysis and interpretation of data, revising the manuscript critically for important intellectual content, and final approval of the version to be submitted.

MN: obtaining the funding, analysis and interpretation of data, revising the manuscript critically for important intellectual content, and final approval of the version to be submitted.

CEL: obtaining the funding, analysis and interpretation of data, revising the manuscript critically for important intellectual content, and final approval of the version to be submitted.

JT: obtaining the funding, analysis and interpretation of data, revising the manuscript critically for important intellectual content, and final approval of the version to be submitted.

TN: obtaining the funding, conception and design of the study, analysis and interpretation of data, revising the manuscript critically for important intellectual content, and final approval of the version to be submitted.

Conflict of Interest: AG is the President of BICL, LLC, and a consultant to MerckSerono, Pfizer, Galapagos, Roche, AstraZeneca and TissueGene. Other authors have nothing to disclose.

was scored at 28 scored locations (14 for cartilage, 6 for menisci, 6 for ligaments, 1 for joint capsule, and 1 popliteal-tibial vessels). A single musculoskeletal radiologist scored cartilage and meniscus subregions, as well as vascular calcifications assigning to each a score ranging from 0–3. The joint capsule, medial and lateral posterior meniscal roots, ACL/PCL and 2 collateral ligaments (MCL/LCL) were each scored 0 or 1 for absence or presence of mineralization. To assess reliability, 31 subject CTs were reread 12 weeks later by the same reader and by a second reader and agreement was evaluated using a weighted kappa.

RESULTS: The intra-reader reliability ranged from 0.92 for ligaments to 1.0 for joint capsule. The inter-reader reliability ranged from 0.94 for cartilage and ligaments, to 1.0 for joint capsule.

CONCLUSION: BUCKS demonstrated excellent reliability and is a potentially useful CT-based tool for studying the role of calcium crystals in knee OA.

INTRODUCTION

Knee osteoarthritis (OA) is the most common form of joint disease in older adults and a leading cause of lower-extremity disability globally^{1,2}, with no effective disease-modifying pharmacologic therapy to date. This is mainly due to the incomplete understanding of the underlying pathogenesis of OA. Intra-articular calcium crystals often co-exist with knee OA; however, their role as a potential contributor to the disease pathogenesis is understudied and unclear³.

There are two main types of calcium crystals, calcium pyrophosphate (CPP) and basic calcium apatite (BCP) crystals, which differ in chemical properties, appearance and presentation and potentially in their role in OA pathogenesis.^{4,5} Some believe crystal deposition is a natural consequence of aging and joint damage⁶, while other have hypothesized that these crystals may play a role in cartilage catabolism through causing release of inflammatory cytokines and matrix metalloproteases⁷. To that extent, calcium crystal deposits may be a novel target for the treatment and prevention of OA.

Radiography is the traditional modality for the detection and diagnosis of intraarticular mineralization. However, the projectional nature of this modality results in limited sensitivity for the detection of crystal calcium deposits. A better assessment of their burden and location may only be achieved with a cross-sectional imaging modality. For instance ultrasonography has been extensively studied for this use^{8–12}. While ultrasound has a much higher sensitivity than radiography for the detection of intraarticular cartilage (84% versus 13%)¹⁰, and similar¹³ to higher¹¹ sensitivity in comparison with CT, it is limited because of its inability to visualize the inner margins of the articular cartilage and soft tissues deep to bone surfaces, such as the cruciate ligaments⁹, as well as being operator dependent. Ultrasound would thus be difficult to implement in large scale cohort studies due to its operator dependency, and therefore possible inconsistencies in longitudinal follow-ups. Traditional MRI pulse sequences are also limited in sensitivity and in their ability to distinctly identify calcified cartilage from other abnormalities, such as meniscal tears^{14,15}. CT is the most appropriate imaging modality for this use, attributable to its isotopic three-dimensional reformatting capabilities and excellent soft tissue-mineralization contrast resolution. A feasibility study showed CT can detect and localize mineralization in the knee

to a greater extent than concurrent radiographs, however it did not assess the reliability of a semiquantitative assessment of the burden of intraarticular mineralization using an ordinal scale¹⁶. The aim of this work is to describe and assess the reliability of a novel CT scoring system, the Boston University Calcium Knee Score (BUCKS) method, for assessing the burden and determining the localization of intra-articular mineralization.

METHODS:

We included subjects from the most recent visit of the Multicenter Osteoarthritis Study (MOST) Study, a NIH-funded cohort study of community-dwelling older adults with or at risk of knee OA. All subjects underwent CT scans of bilateral knees.

CT SCANNING PROTOCOL

Examinations were performed at the University of Alabama at Birmingham and at the University of Iowa by using dual energy CT. A GE Discovery CT750HD scanner was used at the University of Alabama at Birmingham (80/140 kVp, 260mAs, 0.9mm pitch, 0.8s exposure, rotation speed 50ms), while a Siemens SOMATOM Force scanner was used at the University of Iowa (80/150 kVp, 250 mAs, 0.8mm pitch, tin filtration at 150kVp, rotation speed 15ms). For this study, we utilized the 80 kVp images from both sites. The raw projection data were reconstructed using a slice thickness of 0.6mm and a slice interval of 0.3mm with a standard 512 × 512 imaging matrix. Display field-of-view (DFOV) were standardized to approximately 14 cm for each respective knee data set, using the standard kernel (University of Alabama at Birmingham) and Qr40 kernel (University of Iowa). The DFOV provided an in-plane resolution of 0.3mm (x plane) × 0.3mm (y plane) which corresponded to an isotropic voxel dimension of 0.3mm × 0.3mm × 0.3mm when using a slice interval of 0.3mm in the z-plane. The CT acquisition covered the distal 20% of femur and proximal 20% of tibia.

RADIOLOGIC SCORING

Each knee was divided into 14 subregions as previously described in the WORMS scoring system¹⁷ (figure 1) for scoring the hyaline articular cartilage, while the medial and lateral menisci were each divided into 3 subregions, resulting in 14 scores for the cartilage, and 6 meniscal scores. Medial and lateral posterior meniscal roots, anterior cruciate ligament (ACL), posterior cruciate ligament (PCL), medial collateral ligament (MCL), lateral collateral ligament (LCL), joint capsule, and popliteal-tibial vessels were also scored.

Each hyaline cartilage subregion was graded for calcium crystals on a 0–3 ordinal scale based on the extent of crystal mineralization (% of surface area as related to the size of each individual region). Grade 0 = none, grade 1 < 10% of region of cartilage surface area, grade 2 = 10–75% of region of cartilage surface area, and grade 3 >75% of region of cartilage surface area (figure 2)¹⁸. An identical scoring system was used for menisci (figure 3). The posterior meniscal root attachments, MCL and LCL, ACL and PCL, and joint capsule were each graded either 0 (absent) or 1 (present) (figures 4–7). For vascular calcifications, we used an ordinal score (0–3) for the extent of mineralization along the popliteal-tibial

vascular axis (Grade 0= normal, grade 1 <25% of the vessel length, grade 2 = 25–50% of the vessel length, and grade 3 > 50% of the vessel length) (figure 8).

A single musculoskeletal radiologist with 8 years of experience in semi-quantitative scoring of knee OA features (MJ) scored CT examinations of both knees of all participants using axial images, along with multiplanar reformats (MPR) in the sagittal and coronal views. The location of calcium deposition and the shape of the structure in which calcium was deposited made it possible to identify the tissue affected.

SELECTION OF IMAGES FOR RELIABILITY READINGS

After the CT scans from the first 300 study participants (598 knees) had been read for the first time by the initial reader (MJ), the statistical distributions of the maximum cartilage and meniscal calcification scores, and the number of subregions affected within each knee were examined. Because of the low prevalence of intraarticular mineralization, we randomly selected 30 knees (from the eligible 598 knees), weighted to include approximately equal numbers of knees with grade 0, grade 1, and grade 2–3 calcifications, based on the initial reading. Contralateral knees were also added to the selection, but one was excluded due to knee arthroplasty and an additional participant (2 knees) was selected to provide a total of 61 knees from 31 participants selected for this reliability study. The Kellgren and Lawrence grade was not taken into account, at any point, for the selection of participants in this reliability study. Twelve weeks later the same reader (MJ) read the scans for a 2nd time for assessment of intra-rater reliability. Another board-certified musculoskeletal radiologist with 19 years of experience in semi-quantitative scoring of knee OA features (AG) independently read the scans for assessment of inter-rater reliability. The selection process is summarized in figure 9.

STATISTICAL ANALYSIS

The intra-rater reliability for grade of intra-articular calcium crystals in specific subregions (hyaline cartilage, meniscal fibrocartilage, ligamentous structures, and vessels) between readings at time-points 1 and 2 was measured by calculating weighted kappa statistics (95% confidence interval) using SAS 9.3 (SAS Inc., NC). The same method was used for inter-rater reliability, between reader 1 (MJ) and reader 2 (AG). Taking clustering into consideration, we used weighted-kappa statistic¹⁹ for agreement on ordinal scores (cartilage, meniscus and vascular mineralization), using Fleiss-Cohen weights, and regular kappa statistic²⁰ for features scored as present/absent (cruciate/collateral ligaments, meniscal roots, and capsule), all at a subregion level, and similarly to previously published reliability study of the WORMS scoring system¹⁷.

The study protocol was approved by the institutional review boards at the University of Iowa, University of Alabama, Birmingham, University of California, San Francisco, and Boston University Medical Center.

RESULTS

The sample demographics and Kellgren and Lawrence grades are presented in table 1. Intra-articular calcium crystals were present on CT images of 50 knees, with 38 having articular

cartilage calcifications and 35 having meniscal calcifications. The reliability of the instrument was assessed on 31 subjects. The intra-rater reliability for the features described above is reported in table 2. It ranged from 0.92 for ligaments to 1.0 for joint capsule. The inter-rater reliability ranged from 0.94 for cartilage and ligaments, to 1.0 for joint capsule. All measures of reliability demonstrated at minimum very good agreement according to the criteria developed by Landis and Koch²¹. Figures 2–7 demonstrate distribution of calcium crystals in cartilage, menisci, ligaments, joint capsule, and vessels.

DISCUSSION

CT is a unique tool allowing the assessment of soft tissue mineralization in the knee. It combines the benefits of a cross-sectional imaging technique with isotropic three-dimensional reconstruction abilities, relatively high resolution, and excellent soft tissue-mineralization contrast. Our study confirms findings from previously published cadaveric²² and *in-vivo*¹⁶ CT studies demonstrating that calcium crystal deposition is ubiquitous, involving not only the cartilage but all components of the joint including menisci, ligaments and capsule.

This report provides data on the reliability of intraarticular calcium deposits scored using BUCKS: a semi-quantitative scoring instrument for CT assessment of soft tissue mineralization in the knee. The proposed subregional delineation is similar to prior MRI-based semi-quantitative scoring tools such as WORMS¹⁷, allowing for possible examination of association and co-localization of features from both imaging tools. Meniscal root attachments were added to this scoring tool due to their increasingly incriminated role in OA²³. While the ligamentous structures are less readily detectable on CT in comparison with MRI, the mineralization-soft tissue contrast provided by calcium crystal deposition makes the shape of such structures readily recognizable.

CT assessment could help identify different patterns of intra-articular calcium crystal deposition in OA. Our findings provide insights into the intriguing possibility that calcification may be a more global phenomenon within the joint than previously recognized. Further, studying the association of intra-articular mineralization with known MRI-detected features may identify new mechanistic risk factors for radiographic and clinical OA. Ultimately this line of inquiry may help elucidate the underlying processes of the pathophysiology and epidemiology of knee OA, and address the long-unanswered question of whether articular calcification is a cause or consequence, or both, of OA pathology.

This scoring system is exploratory in nature and warrants further investigation and validation. Indeed, there are scant data in the literature pertaining to the role of soft tissue mineralization in knee OA^{6,7}. The potential utility of such a tool is underlined by the existing MRI-based semi-quantitative scoring systems which have proven their usefulness in advancing knowledge in the field of knee OA research^{18,24}, especially when applied to large-scale longitudinal cohorts, including the present cohort. While measurement properties (including construct and predictive validity and the responsiveness) will need to be assessed in subsequent studies, we expect correlation with semiquantitative MRI features will further

advance our knowledge of the pathogenesis of knee OA. BUCKS is not intended for clinical use or follow-up of patients with osteoarthritis at this stage.

We acknowledge the concern for radiation exposure as a limitation for this scoring system. However we emphasize that CT examination of the knee carries a much lower effective dose than CT examinations of more proximal body regions. For comparison, the effective dose for CT of the knee reported as 0.15 mSv is dramatically lower than CT of the hip (3mSv). This difference is related to the difference in radiosensitivity of the exposed tissues, and explained by the minimal amount of bone marrow present in the knee region, while bone itself is amongst the least radiosensitive tissues in the body²⁵. The effective dose from a CT of the knee is equivalent to 2 chest radiographs (0.08 mSv per radiograph), and comparable to a round-trip airplane flight London – New York (0.1mSv)²⁵. Also, as an attempt to comply with the ALARA principle (As Low As Reasonably Achievable), both knees were imaged during the same acquisition, keeping the delivered dose unchanged. Considering the low radiation exposure, longitudinal scanning to follow progression of disease can be achieved well below natural background exposure. An additional limitation of the reported scoring system is its inability to distinguish between the different types of calcium crystals. In deed BUCKS is only intended for quantitative assessment of intra-articular burden, rather than qualitative assessment of intraarticular crystal nature. However, because we used dual-energy technology for all participants, this information is available in this cohort and further analysis of data may be able to elucidate the exact nature of calcium crystal deposits, and also differentiate calcium from urate.

In summary, we described a new CT-based scoring tool and assessed its reliability. BUCKS demonstrates excellent intra- and inter-rater reliability. Further studies will determine the validity and responsiveness of this scoring tool, especially in epidemiological studies. The correlation of intra-articular mineralization deposition with other MRI-based semi-quantitative features in large-scale cohorts may lay the groundwork for a better understanding of knee OA pathophysiology and more specifically the role of soft tissue mineralization in this disease.

Supplementary Material

Refer to Web version on PubMed Central for supplementary material.

Acknowledgements:

Funding Sources:

The MOST Study is supported by NIH grants from the National Institute on Aging to Drs. Lewis (U01-AG-18947), Torner (U01-AG-18832), Nevitt (U01-AG-19069), and Felson (U01-AG-18820). This study was also supported by Dr. Neogi (K24 AR070892), and P60 AR047785

REFERENCES

1. Centers for Disease Control and Prevention (CDC). Prevalence of disabilities and associated health conditions among adults--United States, 1999. *MMWR Morb Mortal Wkly Rep.* 2001;50(7):120–125. <http://www.ncbi.nlm.nih.gov/pubmed/11393491>. Accessed February 18, 2019. [PubMed: 11393491]

2. Vos T, Flaxman AD, Naghavi M, et al. Years lived with disability (YLDs) for 1160 sequelae of 289 diseases and injuries 1990–2010: a systematic analysis for the Global Burden of Disease Study 2010. *Lancet*. 2012;380(9859):2163–2196. doi:10.1016/S0140-6736(12)61729-2 [PubMed: 23245607]
3. Derfus BA, Kurian JB, Butler JJ, et al. The high prevalence of pathologic calcium crystals in pre-operative knees. *J Rheumatol*. 2002;29(3):570–574. <http://www.ncbi.nlm.nih.gov/pubmed/11908575>. Accessed February 18, 2019. [PubMed: 11908575]
4. Wise CM. Crystal-associated arthritis in the elderly. *Rheum Dis Clin North Am*. 2007;33(1):33–55. doi:10.1016/j.rdc.2006.12.007 [PubMed: 17367691]
5. Ea H-K, Lioté F. Advances in understanding calcium-containing crystal disease. *Curr Opin Rheumatol*. 2009;21(2):150–157. doi:10.1097/BOR.0b013e3283257ba9 [PubMed: 19339926]
6. Mitsuyama H, Healey RM, Terkeltaub RA, Coutts RD, Amiel D. Calcification of human articular knee cartilage is primarily an effect of aging rather than osteoarthritis. *Osteoarthr Cartil*. 2007;15(5):559–565. doi:10.1016/j.joca.2006.10.017
7. Ea H-K, Nguyen C, Bazin D, et al. Articular cartilage calcification in osteoarthritis: Insights into crystal-induced stress. *Arthritis Rheum*. 2011;63(1):10–18. doi:10.1002/art.27761 [PubMed: 20862682]
8. Foldes K Knee chondrocalcinosis: an ultrasonographic study of the hyalin cartilage. *Clin Imaging*. 26(3):194–196. <http://www.ncbi.nlm.nih.gov/pubmed/11983473>. Accessed February 19, 2019.
9. Sofka CM, Adler RS, Cordasco FA. Ultrasound diagnosis of chondrocalcinosis in the knee. *Skeletal Radiol*. 2002;31(1):43–45. doi:10.1007/s002560100434 [PubMed: 11807593]
10. Ellabban AS, Kamel SR, Omar HASA, El-Sherif AMH, Abdel-Magied RA. Ultrasonographic diagnosis of articular chondrocalcinosis. *Rheumatol Int*. 2012;32(12):3863–3868. doi:10.1007/s00296-011-2320-1 [PubMed: 22193232]
11. Barskova VG, Kudaeva FM, Bozhieva LA, Smirnov AV, Volkov AV, Nasonov EL. Comparison of three imaging techniques in diagnosis of chondrocalcinosis of the knees in calcium pyrophosphate deposition disease. *Rheumatology (Oxford)*. 2013;52(6):1090–1094. doi:10.1093/rheumatology/kes433 [PubMed: 23382359]
12. Filippou G, Adinolfi A, Iagnocco A, et al. Ultrasound in the diagnosis of calcium pyrophosphate dihydrate deposition disease. A systematic literature review and a meta-analysis. *Osteoarthr Cartil*. 2016;24(6):973–981. doi:10.1016/J.JOCA.2016.01.136
13. Gruber M, Bodner G, Rath E, Supp G, Weber M, Schueller-Weidekamm C. Dual-energy computed tomography compared with ultrasound in the diagnosis of gout. *Rheumatology*. 2014;53(1):173–179. doi:10.1093/rheumatology/kes341 [PubMed: 24136065]
14. Burke BJ, Escobedo EM, Wilson AJ, Hunter JC. Chondrocalcinosis mimicking a meniscal tear on MR imaging. *AJR Am J Roentgenol*. 1998;170(1):69–70. doi:10.2214/ajr.170.1.9423602 [PubMed: 9423602]
15. Disler DG, McCauley TR, Kelman CG, et al. Fat-suppressed three-dimensional spoiled gradient-echo MR imaging of hyaline cartilage defects in the knee: comparison with standard MR imaging and arthroscopy. *AJR Am J Roentgenol*. 1996;167(1):127–132. doi:10.2214/ajr.167.1.8659356 [PubMed: 8659356]
16. Misra D, Guermazi A, Sieren JP, et al. CT imaging for evaluation of calcium crystal deposition in the knee: initial experience from the Multicenter Osteoarthritis (MOST) study. *Osteoarthr Cartil*. 2015;23(2):244–248. doi:10.1016/j.joca.2014.10.009
17. Peterfy C, Guermazi A, Zaim S, et al. Whole-Organ Magnetic Resonance Imaging Score (WORMS) of the knee in osteoarthritis. *Osteoarthr Cartil*. 2004;12(3):177–190. doi:10.1016/j.joca.2003.11.003
18. Hunter DJ, Guermazi A, Lo GH, et al. Evolution of semi-quantitative whole joint assessment of knee OA: MOAKS (MRI Osteoarthritis Knee Score). *Osteoarthr Cartil*. 2011;19(8):990–1002. doi:10.1016/j.joca.2011.05.004
19. Yang Z, Zhou M. Kappa statistic for clustered matched-pair data. *Stat Med*. 2014;33(15):2612–2633. doi:10.1002/sim.6113 [PubMed: 24532251]
20. Zhou M, Yang Z. A note on the kappa statistic for clustered dichotomous data. *Stat Med*. 2014;33(14):2425–2448. doi:10.1002/sim.6098 [PubMed: 24488927]

21. Landis JR, Koch GG. The measurement of observer agreement for categorical data. *Biometrics*. 1977;33(1):159–174. <http://www.ncbi.nlm.nih.gov/pubmed/843571>. Accessed March 12, 2019. [PubMed: 843571]
22. Bastien Touraine S, Korng Ea H, Rie Bousson V, et al. Chondrocalcinosis of Femoro-Tibial and Proximal Tibio-Fibular Joints in Cadaveric Specimens: A High-Resolution CT Imaging Study of the Calcification Distribution. 2013. doi:10.1371/journal.pone.0054955
23. Guermazi A, Hayashi D, Jarraya M, et al. Medial Posterior Meniscal Root Tears Are Associated with Development or Worsening of Medial Tibiofemoral Cartilage Damage: The Multicenter Osteoarthritis Study. *Radiology*. 2013;268(3):814–821. doi:10.1148/radiol.13122544 [PubMed: 23696679]
24. Jarraya M, Hayashi D, Roemer FW, Guermazi A. MR Imaging-based Semi-quantitative Methods for Knee Osteoarthritis. *Magn Reson Med Sci*. 2016;15(2):153–164. doi:10.2463/mrms.rev.2015-0058 [PubMed: 26632537]
25. Biswas D, Bible JE, Bohan M, Simpson AK, Whang PG, Grauer JN. Radiation Exposure from Musculoskeletal Computerized Tomographic Scans. *J Bone Jt Surgery-American Vol*. 2009;91(8):1882–1889. doi:10.2106/JBJS.H.01199

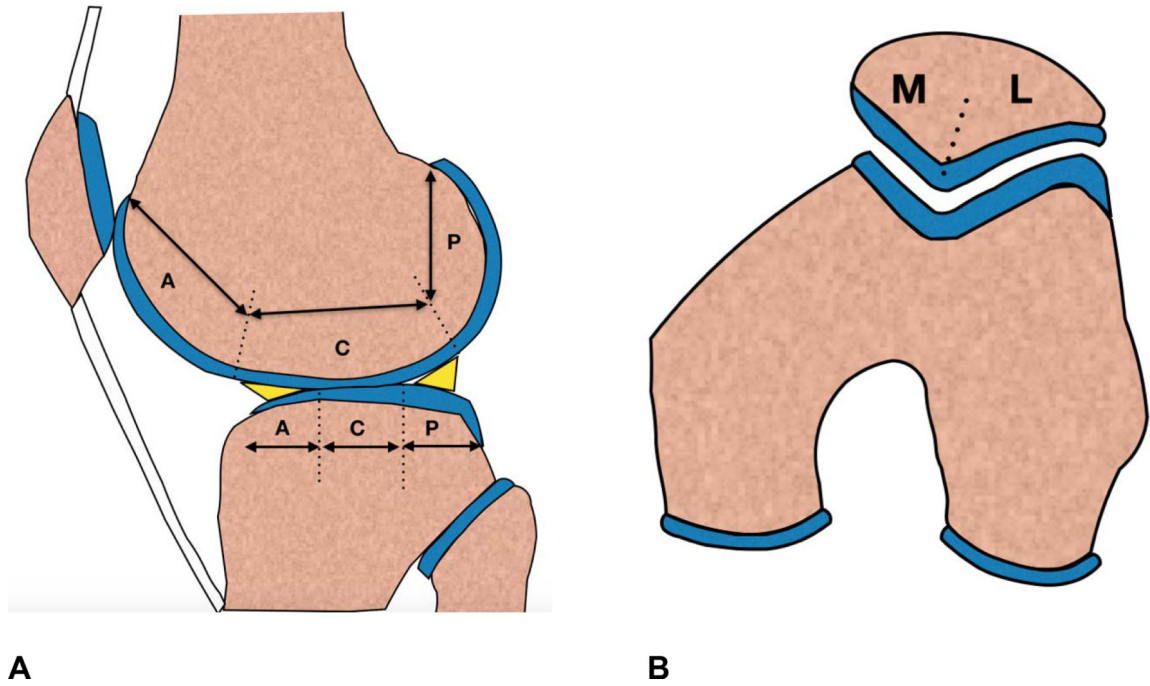


Figure 1. Schematics representing (A) a sagittal view of the knee helps explain the 12 subregions of the medial and lateral tibiofemoral joints (C: central, A: Anterior, and P: Posterior), and (B) an axial view of the knee showing the 2 medial and lateral patellar subregions (M: Medial, and L: Lateral).

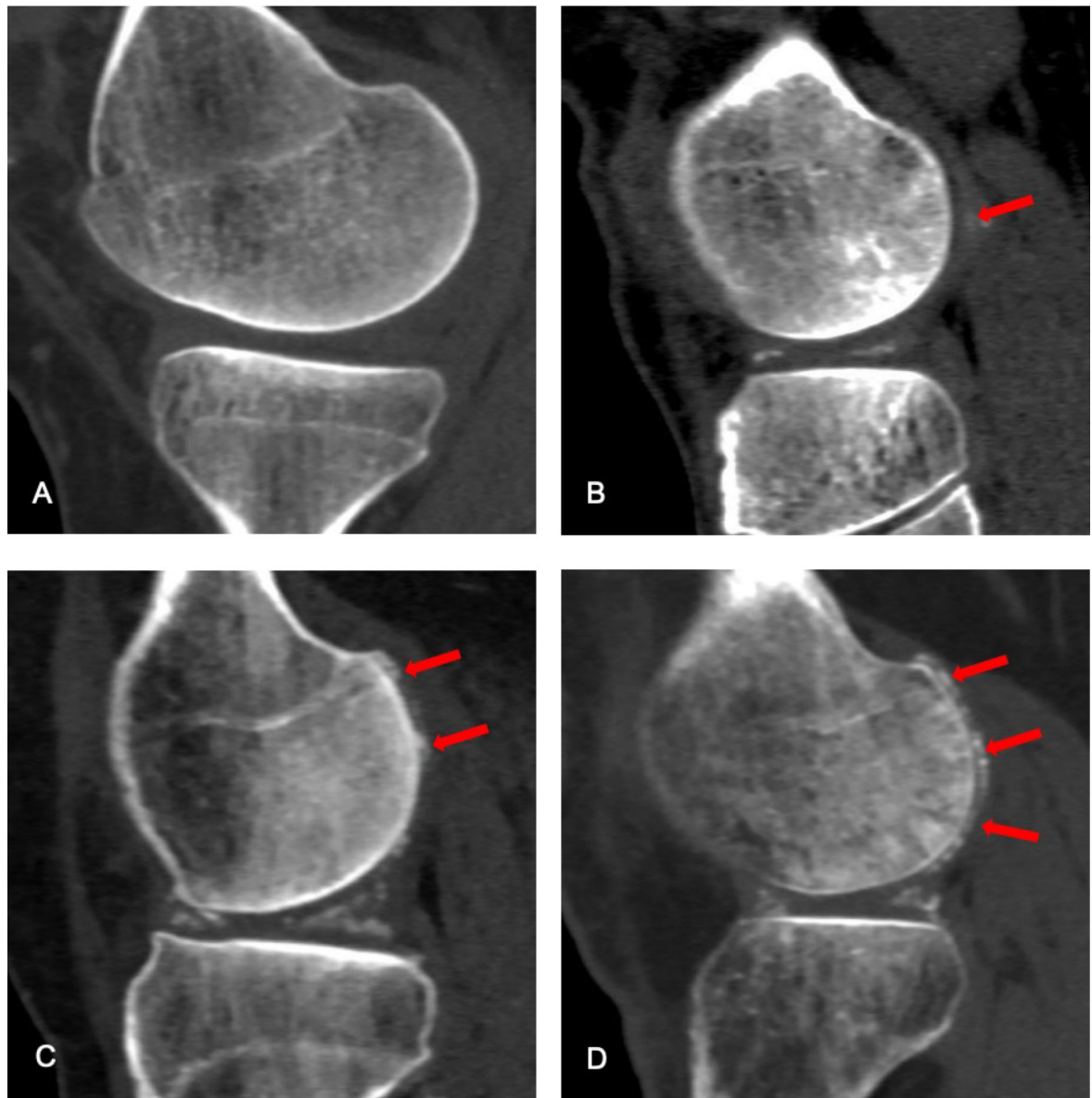


Figure 2. Cartilage mineralization grading. Grade 0= none, grade 1<10% of subregional surface grade 2= 10–75% of the subregional surface, grade 3 >75% of the subregional surface. (A–D) Sagittal computed tomography reformats. (A) Grade 0 with no cartilage mineralization in posterior subregion of medial femur. (B) Grade 1 cartilage mineralization is depicted in posterior subregion of lateral femur (arrow). (C) Grade 2 cartilage mineralization in the posterior subregion of the lateral femur (arrows). D. Grade 3 cartilage mineralization is depicted in posterior subregion of lateral femur (arrows).

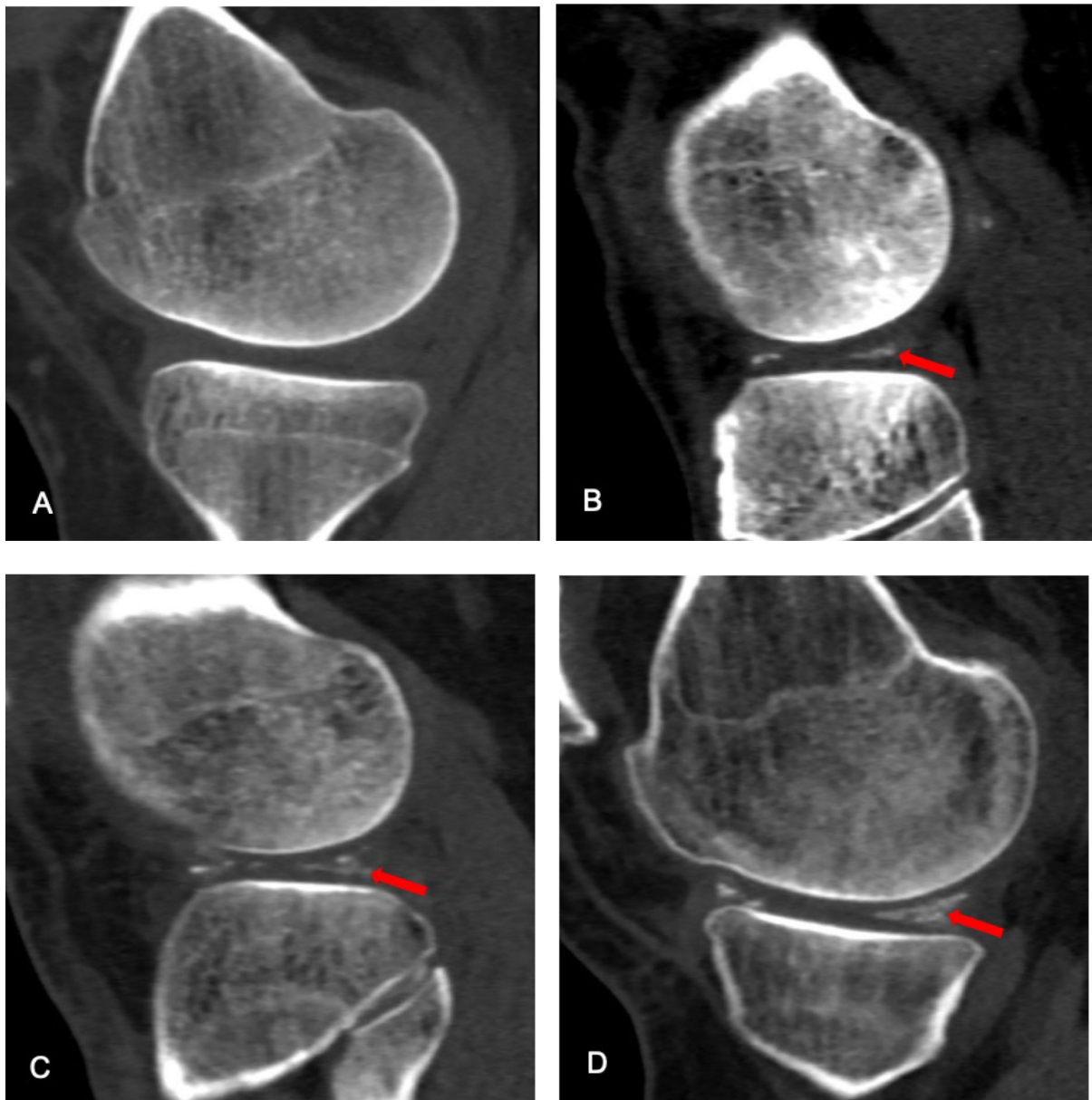


Figure 3. Meniscal mineralization grading. Grade 0= none, grade 1<10% of subregional volume grade 2= 10–75% of the subregional volume, grade 3 >75% of the subregional volume. (A-D) Sagittal computed tomography reformats. (A) Grade 0 with no meniscal crystal deposition in the posterior horn of the medial meniscus. (B) Grade 1 meniscal mineralization in the posterior horn of lateral meniscus (arrow). (C) Grade 2 meniscal mineralization in the posterior horn of the lateral meniscus (arrow). D. Grade 3 cartilage mineralization in the posterior horn of the medial meniscus (arrow).

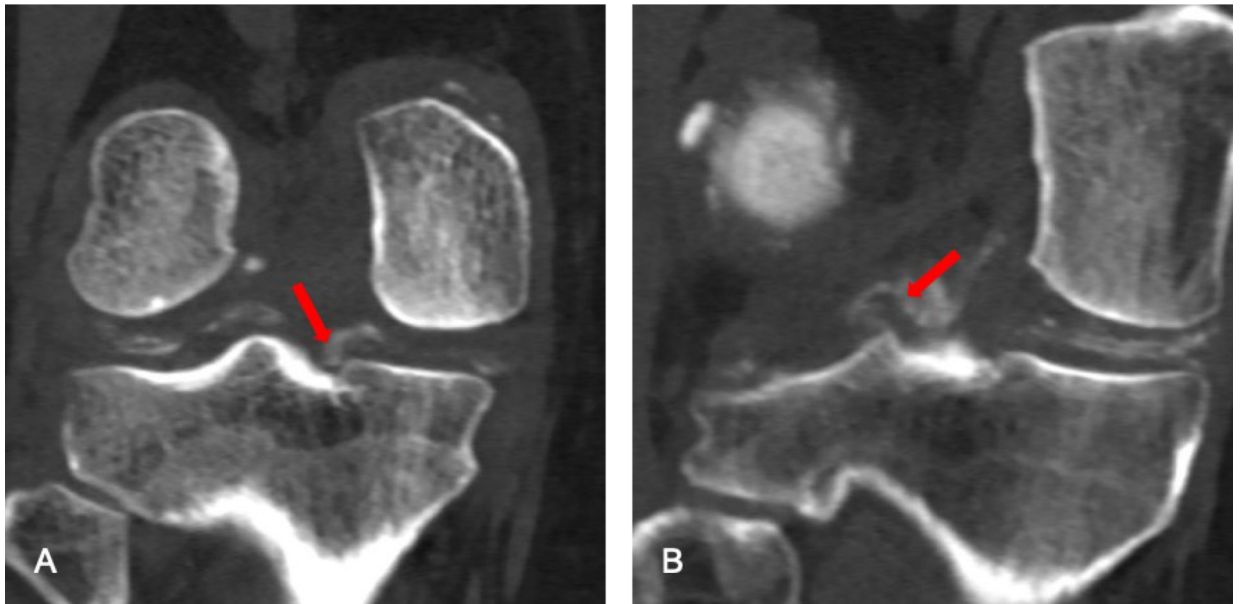


Figure 4. Mineralization grading of the posterior meniscal roots. Grade 0= none, grade 1= present. (A,B) Coronal computed tomography reformats. (A) Grade 1 mineralization of the posterior medial meniscus root, with calcium crystal deposition following the shape of the same structure (arrow). (B) Grade 1 mineralization of the posterior lateral meniscus root (arrow).

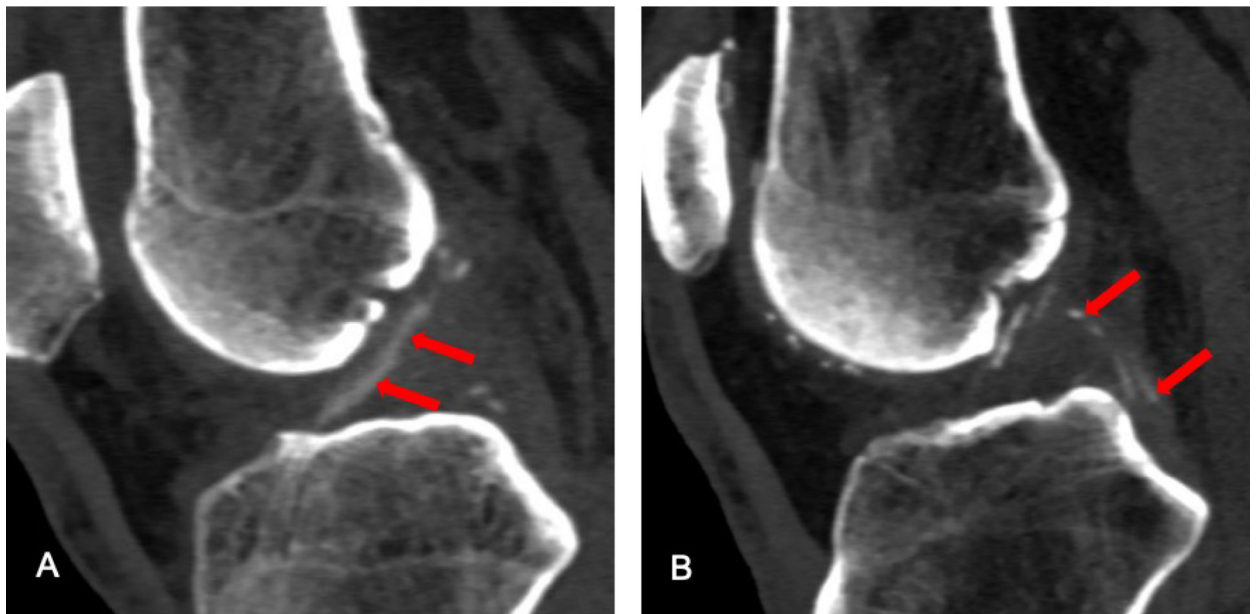


Figure 5. Mineralization grading of the cruciate ligaments. Grade 0= none, grade 1= present. (A,B) Sagittal computed tomography reformats. (A) Grade 1 mineralization of the ACL with calcium crystal deposition following the shape of the ACL (arrows). (B) Grade 1 mineralization of the PCL with calcium crystal deposition follows the shape of the PCL (arrows).

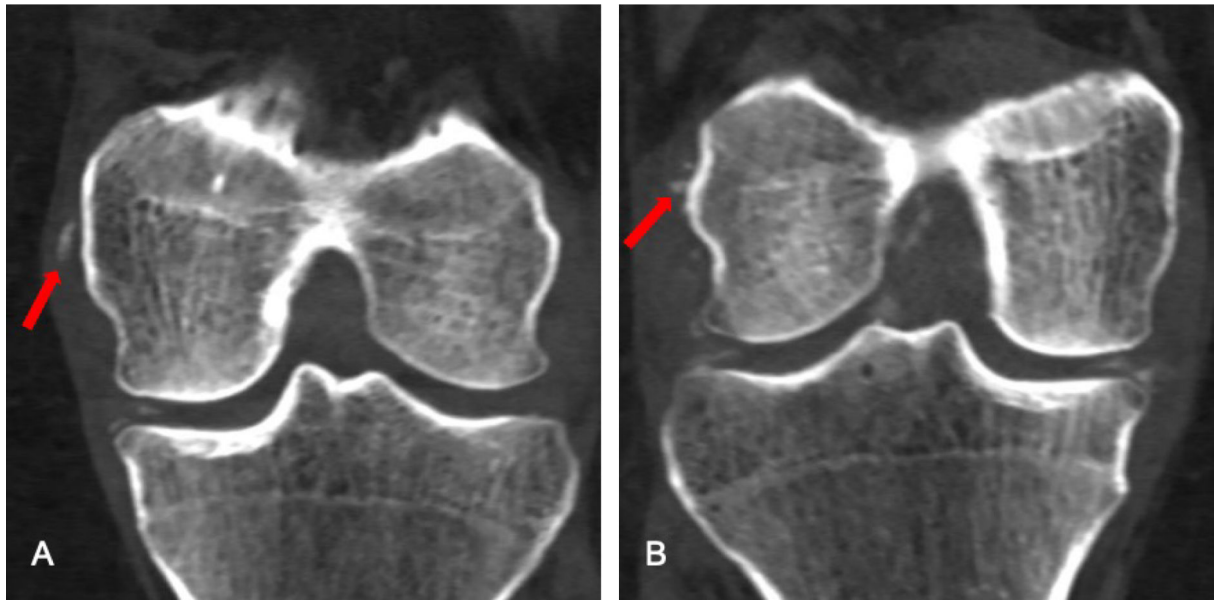


Figure 6. Mineralization grading of the collateral ligaments. Grade 0= none, grade 1= present. (A,B) Coronal computed tomography reformats. (A) Grade 1 mineralization of the medial collateral ligament, with calcium crystal deposition following the shape of the same structure (arrow). (B) Grade 1 mineralization of the lateral collateral ligament (arrow).

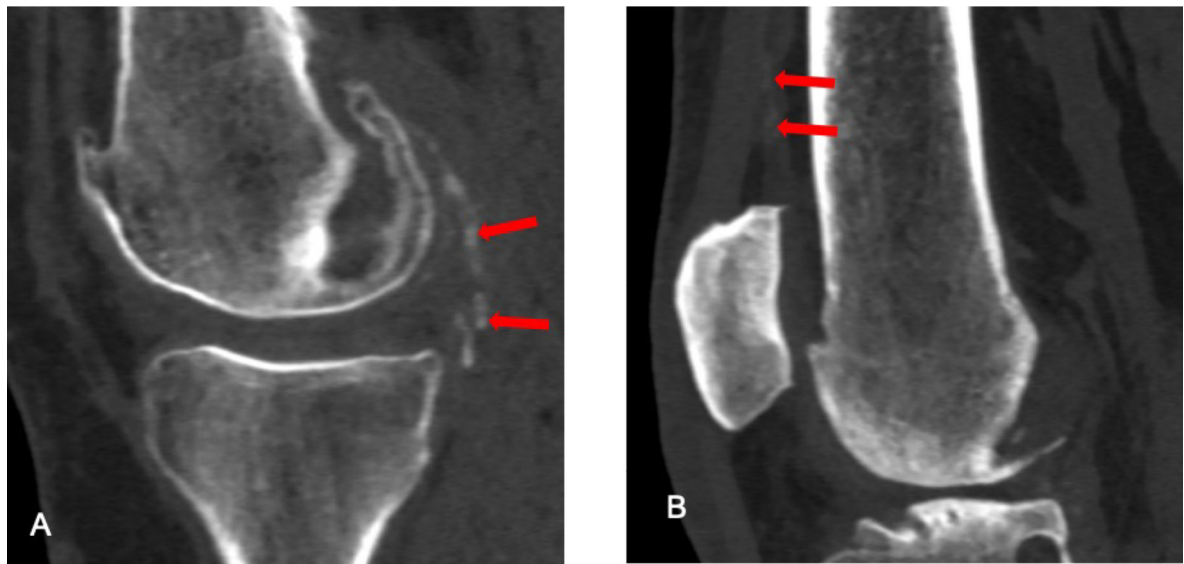


Figure 7. Mineralization grading of the joint capsule. Grade 0 = none, grade 1 = present. (A,B) Sagittal computed tomography reformats. (A) Grade 1 mineralization of the joint capsule along the posterior medial femoral condyle (arrows). (B) Another example of grade 1 mineralization of the joint capsule in the suprapatellar pouch (arrow).

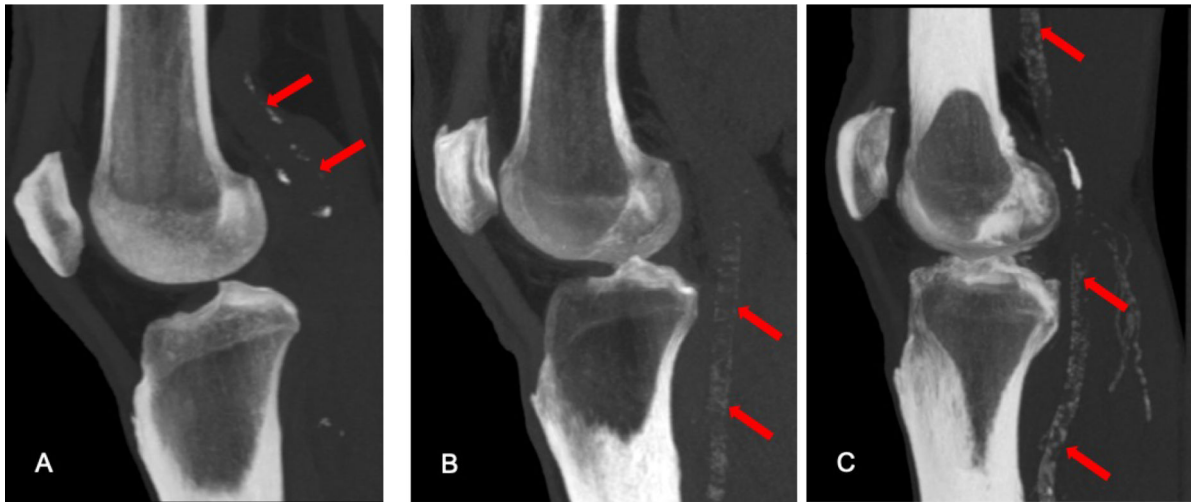


Figure 8.

Vascular calcification grading. Grade 0 = none, grade 1 <25% of the popliteal-tibial vascular length, grade 2 = 25–50% of the popliteal-tibial vascular length, grade 3 >50% of the popliteal-tibial vascular length. (A–C) Sagittal maximum intensity projection computed tomography reformats. (A) Grade 1 vascular calcifications <25% of the popliteal-tibial vascular length (arrows). (B) Grade 2 vascular calcifications, 25–50% of the popliteal-tibial vascular length (arrows). (C) Grade 3 vascular calcifications >50% of the popliteal-tibial vascular length (arrows).

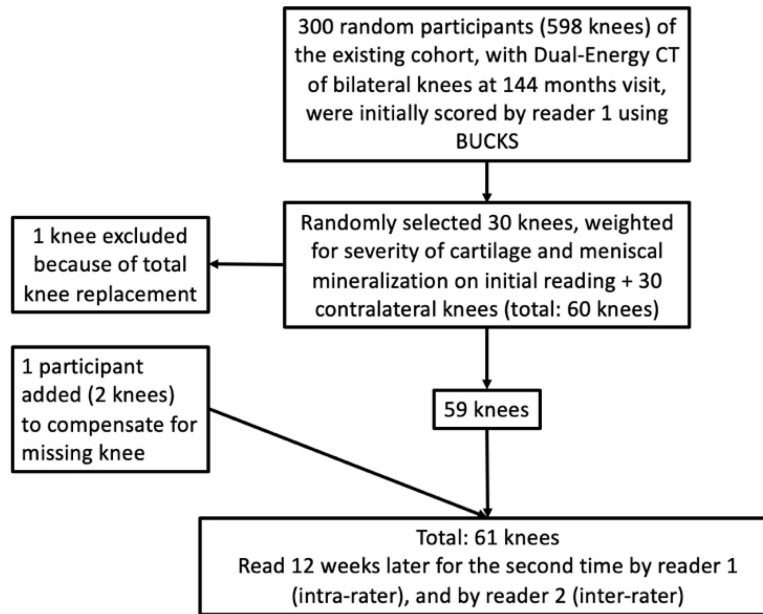


Figure 9.
Flow chart of the selection process for the reliability study.

Table 1:

Sample demographics and knee Kellgren and Lawrence grades

Female (%)	19 (61.3)		
BMI * (standard deviation)	31.1 (5.2)		
Age (standard deviation)	72.2 (6.6)		
Tibiofemoral Kellgren and Lawrence (KL) Grading	Index knees (n = 31)	Contralateral knees (n = 30)	Total (n = 61)
KL Grade 0 (%)	7	6	13
KL Grade 1 (%)	6	8	14
KL Grade 2 (%)	10	5	15
KL Grade 3 (%)	6	8	14
KL Grade 4 (%)	1	2	3
Unscorable (total knee replacement)	0	1 (excluded)	NA
Not available	1	1	2

* BMI in kg/m²

Table 2.

Intra- and inter-rater reliability at the subregion levels of the knee.

Tissue Compartments	Kappa Weighted Reliability [95% Confidence Interval]	
	Intra-rater	Inter-rater
Hyaline Cartilage (854 subregions = 14 locations × 61 knees)	0.96 [0.94– 0.98]	0.94 [0.91 – 0.97]
Meniscus * (488 subregions = 8 locations × 61 knees)	0.99 [0.98 – 1.00]	0.97 [0.95 – 0.99]
Ligaments (244 subregions = 4 locations × 61 knees)	0.92 [0.86 – 0.99]	0.94 [0.88 – 1.00]
Capsule (1 location × 61 knees)	1.00 [1.00 – 1.00]	1.00 [1.00 – 1.00]
Vessels (1 location × 61 knees)	0.98 [0.96 – 1.00]	0.98 [0.95 – 1.00]

* Including posterior meniscal roots.

Author Manuscript

Author Manuscript

Author Manuscript

Author Manuscript